Supplementary material for: "Heat transfer by rapidly rotating Rayleigh-Bénard convection"

E. M. KING[1], S. STELLMACH[2], AND J. M. AURNOU[3]

[1]Department of Earth and Planetary Science, University of California, Berkeley, 94720-4767 USA

[2]Institut für Geophysik, WWU Münster, AG Geodynamik Corrensstr. 24, Münster, 48149 Germany

[3]Department of Earth and Space Sciences, University of California, Los Angeles, 90095-1567 USA

(Received February 2, 2011)

Here, we provide supplementary material on the experimental methods for "Heat transfer by rapidly rotating Rayleigh-Bénard convection". Section 1 provides a detailed description of the laboratory experiment, and section 2 tabulates heat transfer data from laboratory.

1. Laboratory Experiments

1.1. *Experimental Apparatus*

Laboratory experiments are carried out in cylindrical tanks of water or sucrose solution using the rotating magnetoconvection device (RoMag) at UCLA (King 2009). The experimental convection setup is shown in figure 1, and consists of a cylindrical convection tank that sits atop a rotating pedestal. The convection tank is 20 cm in diameter, and has variable height, from 3.2 cm to 20 cm such that the diameter to height aspect ratio is in the range $1 \leq \Gamma \leq 6.25$. Increasing the tank's height increases Ra (as h^3) and decreases E (as h^{-2}).

The tank is heated from below by an electrical heating element and cooled from above by a thermstated heat exchanger. The bottom thermal boundary condition is therefore one of constant heat flux, rather than of constant temperature, as in the numerical simulations. This means that, experimentally, we fix flux-Rayleigh numbers, $Rf = RaNu$, instead of the traditional Rayleigh numbers that are fixed in the numerical simulations. Despite this difference in boundary conditions, mean convective behavior does not strongly vary between the two types of thermal boundary conditions (e.g., Johnston & Doering 2009; King *et al.* 2009).

Convection experiments are carried out near room temperature and the apparatus is surrounded by roughly 20 cm of closed cell foam insulation to minimize ambient thermal interaction. The cylinder sidewalls are polycarbonate, and the top and bottom tank endwalls are thin layers of either copper or aluminum, designed to minimize thermal heterogeneity within the boundaries. The importance of finite conductivity is characterized by the Biot number, $Bi = Nu \frac{k_{\text{fluid}}}{H_{\text{fluid}}} \frac{H_{\text{boundary}}}{k_{\text{boundary}}}$, where k is thermal conductivity and H is layer thickness. For the experiments presented here, $Bi < 0.1$, such that the influence of finite conductivity boundaries is small (Verzicco 2004).

Figure 2 shows a schematic of the heat delivery and removal system to the experimental apparatus. The heat required to drive convection is accomplished by a 16 Ohm mica

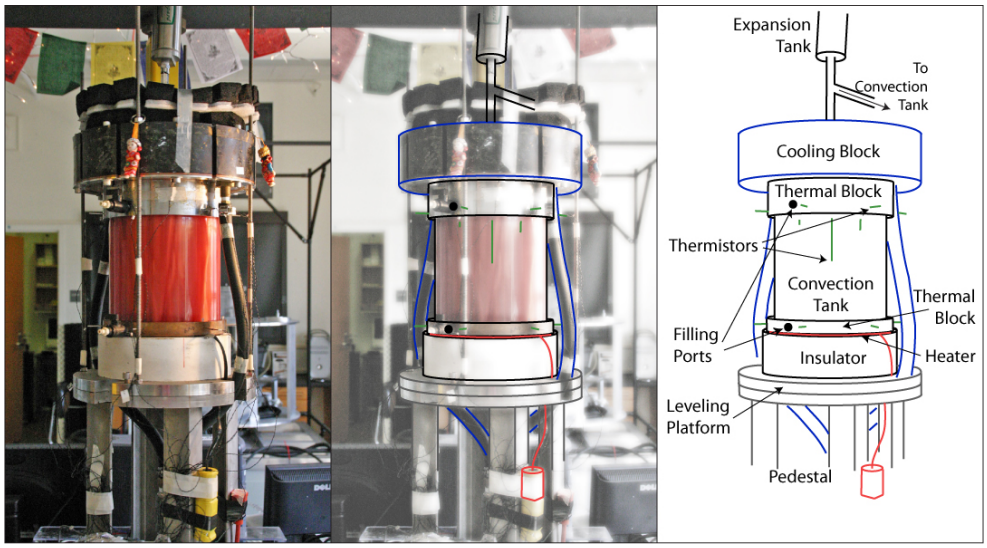

FIGURE 1. The convection tank setup of the rotating magnetoconvection device (RoMag). From bottom to top are the rotating pedestal, leveling platform, insulator, heater, bottom endwall, sidewall, top endwall, cooling block, and expansion tank.

resistance element. A direct current is passed through the heater by way of a 0-5 kW power supply, and is transmitted to the rotating frame by a system of 50 Amp solid-state slip rings. The heat produced below the convection tank is removed above the tank by a heat exchanging unit, referred to as the cooling block. Water is forced through the cooling block by a lab chiller that maintains a reservoir of treated water at a thermostated temperature. The chilled water is delivered into the rotating frame via a two-channel fluid rotary union. The cooling block is an aluminum (T6061) cylinder into which has been cut two double-wound spiral flow channels, such that the temperature distribution is roughly uniform. The heat absorbed by the lab chiller is removed by recirculation from an air-cooled industrial rooftop chiller.

The convection tank setup is rotated by a brushless (for rotation rate uniformity) servomotor. A lower table supporting the diagnostic instrumentation co-rotates such that sensitive signals need not be transmitted through noise inducing slip rings. The rotation rate is limited to 50 rotations per minute, such that the maximum strength of centrifugation within the convection container is never more than 30% gravitational acceleration (Lopez & Marques 2009).

1.2. *Fluid Properties*

Working fluids are water and sucrose solution, whose typical thermophysical properties are listed in Table 1, and the temperature dependence thereof is given below.

The properties of water, in SI units (given in table 1), are (Lide 2000):

$$\rho = 999.8 + 0.1041T - 9.718 \times 10^{-3}T^2 + 5.184 \times 10^{-5}T^3 \tag{1.1}$$

$$\alpha_T = -6.82 \times 10^{-5} + 1.70 \times 10^{-5}T - 1.82 \times 10^{-7}T^2 + 1.05 \times 10^{-9}T^3 \tag{1.2}$$

$$\kappa = 1.31210^{-7} + 6.97210^{-10}T - 5.63110^{-12}T^2 + 2.63310^{-14}T^3 \tag{1.3}$$

$$k = 0.5529 + 2.66210^{-3}T - 2.37410^{-5}T^2 + 1.10810^{-7}T^3 \tag{1.4}$$

$$C_P = \frac{k}{\rho\kappa}, \tag{1.5}$$

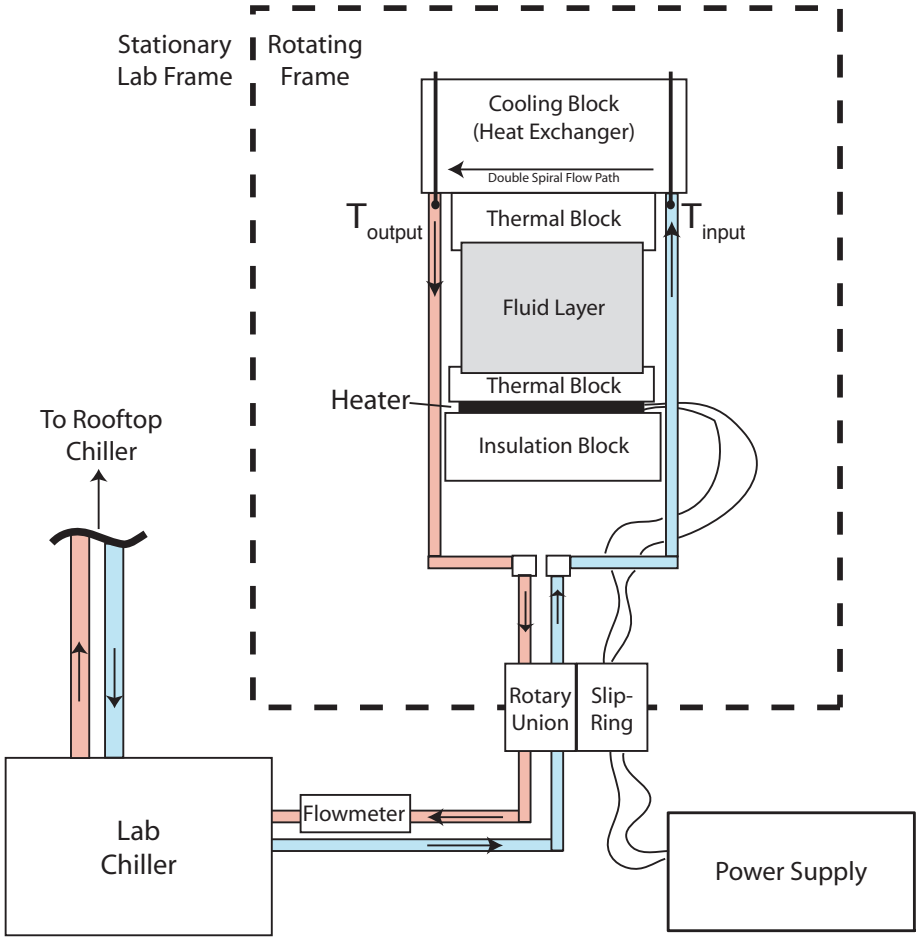

FIGURE 2. A schematic of RoMag's experimental thermal circulation system.

Property	Symbol	Units	Water	Sucrose Solution
density	ρ	$\mathrm{kg/m^3}$	1000	1050
thermal expansivity	α_T	$\mathrm{K^{-1}}$	2×10^{-4}	2×10^{-4}
viscous diffusivity	ν	$\mathrm{m^2/s}$	10^{-6}	1.5×10^{-6}
thermal diffusivity	κ	$\mathrm{m^2/s}$	1.4×10^{-7}	1.4×10^{-7}
Prandtl number	$Pr = \nu/\kappa$	—	7	11
specific heat	Cp	J/kg K	4180	3815
thermal conductivity	k	J/m s K	0.6	0.6

TABLE 1. Thermophysical properties of water (20°C) (Lide 2000) and sucrose solution (14.4% sugar by mass, 20°C) (Hirst & Cox 1976).

where T is the temperature of the fluid in °C.

In some convection cases, sugar is added to water to create a denser solution, which permits polystyrene micro-particles to remain in suspension for use with acoustic Doppler velocimetry. The properties of sucrose solution are essentially that of water with the added dependency of the concentration of sugar. By mass, the percentage of sugar to water in the solution is referred to as degrees Brix, °BX. The density of the solution is measured prior to conducting experiments, and variations about that density with temperature are assumed to be determined by the thermal expansivity of pure water given above. The remaining fluid properties of sucrose solution are (Hirst & Cox 1976):

$$\nu = (6.581/(((61.5 + T) - (1 + 0.011\,T)\,^{\circ}\mathrm{BX})^2))/\rho \tag{1.6}$$

$$\kappa = \frac{k}{\rho C_P} \tag{1.7}$$

$$k = 0.5758 + 1.360 \times 10^{-3}\,T - 3.006 \times 10^{-3}\,^{\circ}\mathrm{BX} - 2.511 \times 10^{-6}\,^{\circ}\mathrm{BX}\,T \\ -3.341 \times 10^{-6}\,^{\circ}\mathrm{BX}^2 - 1.182 \times 10^{-7}\,^{\circ}\mathrm{BX}^2\,T \tag{1.8}$$

$$Cp = [1 - (0.632 - 0.001\,T)\,^{\circ}\mathrm{BX}/100]4184. \tag{1.9}$$

1.3. *Experimental Diagnostics*

Six thermistors are situated within each of the top and bottom boundaries, 2 mm from the fluid interface, at two-thirds the tank's radius. The probes are equally spaced in azimuth, forming six vertically aligned pairs. These thermistors measure the temperature difference across the fluid layer, ΔT. The heat flux, q, is measured as the power input to the resistor, and is compared, for accuracy, with the heating rate of coolant cycling through a thermostated bath atop the convection tank.

Figure 3 shows an example of temperature time series measurements from RoMag. Panels a) and b) show raw thermistor measurements from the top and bottom boundaries, respectively. These temperature measurements are denoted $T_i^{\mathrm{top}}(t)$ and $T_i^{\mathrm{bottom}}(t)$, where $i = 1, ..., 6$ corresponding to azimuthal location. From these measurements are calculated, for example, the mean fluid temperature, T_{fluid} (panel c)), and temperature drop, ΔT (panel d)). The mean temperature of the convecting fluid is calculated as

$$T_{\mathrm{fluid}} = \frac{1}{12}\left\langle \sum_{i=1}^{6} T_i^{\mathrm{top}}(t) + \sum_{i=1}^{6} T_i^{\mathrm{bottom}}(t) \right\rangle_t, \tag{1.10}$$

where $\langle\cdot\rangle_t$ represents time averaging. The mean temperature drop across the fluid layer is calculated as:

$$\Delta T = \frac{1}{6}\left\langle \sum_{i=1}^{6} T_i^{\mathrm{bottom}}(t) - \sum_{i=1}^{6} T_i^{\mathrm{top}}(t) \right\rangle_t. \tag{1.11}$$

2. Laboratory Data

Here, we provide a table of heat transfer data from laboratory experiments. The column headings have the following meaning: h is the height of the convection tank in meters; RPM is the rotation rate of the tank in rotations per minute; Power is the electrical power supplied to the heater in watts; Pr is the Prandtl number of the fluid; E is the Ekman number; Ra is the Rayleigh number; and Nu is the Nusselt number. Non-dimensional parameters are defined as $Pr = \nu/\kappa$, $E = \nu/2\Omega h^2$, $Ra = \alpha_T g \Delta T h^3/\nu\kappa$, and $Nu = qh/k\Delta T$, where ν is the fluid's kinematic viscosity, κ is the fluid's thermal

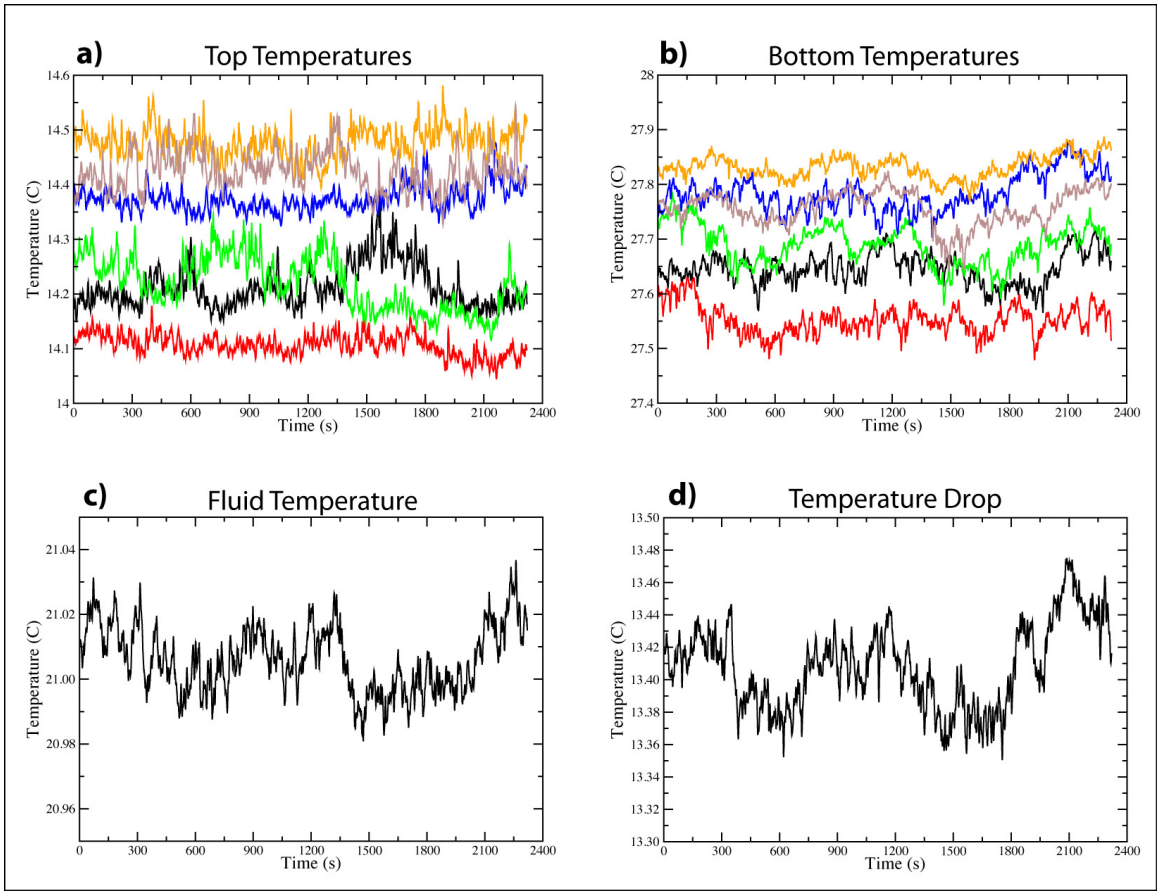

FIGURE 3. Sample temperature time series measurements from non-rotating convection in a 5 cm tank of water with 100 W heat power applied. **a)** and **b)** are temperature time series measurements from the top and, bottom thermistors, respectively, $T_i^{\text{top}}(t)$ and $T_i^{\text{bottom}}(t)$. **c)**: The thermistor measurements from **a)** and **b)** are averaged to calculate a time series measurement of the mean fluid temperature, $T_{\text{fluid}}(t) = \frac{1}{12}\sum_{i=1}^{6}\left(T_i^{\text{top}}(t) + \sum_{i=1}^{6} T_i^{\text{bottom}}(t)\right)$. **d)**: The difference between mean top and bottom temperatures gives the temperature drop, $\Delta T(t) = \frac{1}{6}\left(\sum_{i=1}^{6} T_i^{\text{bottom}}(t) - \sum_{i=1}^{6} T_i^{\text{top}}(t)\right)$. These measurements are then averaged in time for each convection case, and used to calculate fluid properties and nondimensional parameters.

diffusivity, Ω is angular rotation rate, h is the height of the container, α_T is the fluid's thermal expansivity, g is gravitational acceleration, ΔT is the temperature drop across the convection tank, q is heat flux, and k is the fluid's thermal conductivity. Water is the working fluid for all cases but those with h = 9.8 cm, in which sucrose solution was used.

h (m)	RPM	Power (W)	Pr	E	Ra	Nu
0.032	0	10.82	6.946	∞	1.071×10^{6}	8.189
0.032	0	30.48	6.957	∞	2.352×10^{6}	10.47
0.032	0	50.59	6.989	∞	3.479×10^{6}	11.62
0.032	0	100.4	7.051	∞	5.835×10^{6}	13.44
0.032	0	149.6	6.951	∞	8.237×10^{6}	14.7
0.032	0	199.9	6.459	∞	1.183×10^{7}	16.18
0.032	0	299.5	5.786	∞	1.953×10^{7}	18.44
0.032	4.66	10.85	6.933	9.941×10^{-4}	9.545×10^{5}	9.251
0.032	4.66	50.65	7.098	1.015×10^{-3}	3.026×10^{6}	12.86
0.032	4.66	100.6	6.416	9.284×10^{-4}	6.259×10^{6}	15.61
0.032	4.66	200.2	6.812	9.787×10^{-4}	9.836×10^{6}	17.28
0.032	46.63	10.82	6.767	9.724×10^{-5}	2.703×10^{6}	3.451
0.032	46.63	30.48	6.851	9.83×10^{-5}	4.083×10^{6}	6.253
0.032	46.63	50.6	6.738	9.687×10^{-5}	5.275×10^{6}	8.351
0.032	46.63	100.6	7.081	1.012×10^{-4}	6.842×10^{6}	11.37
0.032	46.63	200.3	6.654	9.581×10^{-5}	1.126×10^{7}	15.94
0.032	46.63	299.9	5.916	8.636×10^{-5}	1.757×10^{7}	19.64
0.0472	0	10.81	6.75	∞	3.843×10^{6}	11.54
0.0472	0	30.47	6.736	∞	8.567×10^{6}	14.67
0.0472	0	50.59	6.84	∞	1.251×10^{7}	16.09
0.0472	0	75.06	6.829	∞	1.704×10^{7}	17.6
0.0472	0	100.3	6.808	∞	2.14×10^{7}	18.85
0.0472	0	200.4	6.349	∞	4.183×10^{7}	22.54
0.0472	0	299.2	5.446	∞	7.318×10^{7}	26.12
0.0472	0	398.9	4.824	∞	1.123×10^{8}	28.2
0.0472	1.91	10.85	6.738	1.087×10^{-3}	3.439×10^{6}	13.01
0.0472	1.91	50.35	6.789	1.094×10^{-3}	1.157×10^{7}	17.63
0.0472	1.91	101.1	6.907	1.111×10^{-3}	1.969×10^{7}	19.96
0.0472	1.91	300.6	5.68	9.348×10^{-4}	6.595×10^{7}	26.88
0.0472	19.1	10.49	6.841	1.102×10^{-4}	4.22×10^{6}	9.895
0.0472	19.1	30.8	6.888	1.108×10^{-4}	7.597×10^{6}	15.87
0.0472	19.1	50.27	6.967	1.12×10^{-4}	1.029×10^{7}	18.6
0.0472	19.1	75.21	6.973	1.12×10^{-4}	1.372×10^{7}	20.84
0.0472	19.1	101	6.98	1.121×10^{-4}	1.709×10^{7}	22.42
0.0472	19.1	200.2	6.823	1.099×10^{-4}	3.043×10^{7}	26.34
0.0472	19.1	300.6	5.873	9.628×10^{-5}	5.46×10^{7}	30.42
0.0472	19.1	400.6	5.173	8.607×10^{-5}	8.416×10^{7}	33.42
0.0472	47.7	10.5	6.806	4.392×10^{-5}	9.41×10^{6}	4.493
0.0472	47.7	30.53	6.782	4.378×10^{-5}	1.443×10^{7}	8.59
0.0472	47.7	50.7	6.833	4.407×10^{-5}	1.786×10^{7}	11.32
0.0472	47.7	75.76	6.84	4.411×10^{-5}	2.159×10^{7}	13.97

continued on next page

h (m)	RPM	Power (W)	Pr	E	Ra	Nu
0.0472	47.7	101.1	6.97	4.485×10^{-5}	2.42×10^{7}	15.9
0.0472	47.7	200.3	6.462	4.195×10^{-5}	3.999×10^{7}	22.67
0.0472	47.7	301.4	5.72	3.767×10^{-5}	6.255×10^{7}	28.03
0.0472	47.7	400.5	5.122	3.417×10^{-5}	8.868×10^{7}	32.28
0.098	0	20.69	10.59	∞	4.329×10^{7}	26.52
0.098	0	50.65	10.03	∞	9.851×10^{7}	32.45
0.098	0	100.4	9.623	∞	1.82×10^{8}	38.19
0.098	0	200.1	8.803	∞	3.599×10^{8}	46.29
0.098	0	299.6	7.518	∞	6.298×10^{8}	52.92
0.098	0	496.4	5.986	∞	1.358×10^{9}	58.32
0.098	0.5	20.69	10.92	1.512×10^{-3}	3.982×10^{7}	26.69
0.098	0.5	50.65	10.86	1.505×10^{-3}	8.197×10^{7}	32.14
0.098	0.5	101	10.6	1.472×10^{-3}	1.517×10^{8}	36.81
0.098	0.5	249.9	8.578	1.211×10^{-3}	4.543×10^{8}	48.16
0.098	5	20.46	10.68	1.483×10^{-4}	3.735×10^{7}	29.72
0.098	5	51.04	10.93	1.514×10^{-4}	7.547×10^{7}	34.61
0.098	5	101.5	10.75	1.491×10^{-4}	1.361×10^{8}	39.87
0.098	5	201.7	9.353	1.312×10^{-4}	3.212×10^{8}	46.2
0.098	5	497.2	6.158	8.953×10^{-5}	1.22×10^{9}	62.37
0.098	25	21.02	10.62	2.949×10^{-5}	4.121×10^{7}	28.07
0.098	25	50.84	11.01	3.049×10^{-5}	6.864×10^{7}	37.17
0.098	25	100.8	10.69	2.966×10^{-5}	1.218×10^{8}	44.87
0.098	25	199.7	9.808	2.74×10^{-5}	2.472×10^{8}	53.64
0.098	25	497.9	6.458	1.87×10^{-5}	1.008×10^{9}	70.34
0.098	50	20.87	10.6	1.472×10^{-5}	6.278×10^{7}	18.38
0.098	50	31.03	10.73	1.488×10^{-5}	7.574×10^{7}	22
0.098	50	50.91	10.64	1.477×10^{-5}	1.006×10^{8}	27.75
0.098	50	75.95	10.86	1.505×10^{-5}	1.214×10^{8}	32.56
0.098	50	100.8	10.87	1.506×10^{-5}	1.425×10^{8}	36.78
0.098	50	150.8	10.45	1.452×10^{-5}	1.97×10^{8}	43.86
0.098	50	201.2	9.655	1.351×10^{-5}	2.751×10^{8}	50.27
0.098	50	251.2	8.971	1.262×10^{-5}	3.625×10^{8}	55.57
0.098	50	301	8.403	1.189×10^{-5}	4.528×10^{8}	60.53
0.098	50	400	7.382	1.056×10^{-5}	6.82×10^{8}	67.29
0.098	50	499.5	6.55	9.469×10^{-6}	9.522×10^{8}	73.04
0.098	50	599	5.855	8.552×10^{-6}	1.281×10^{9}	77.12
0.197	0	10.82	6.852	∞	2.989×10^{8}	43.54
0.197	0	30.73	6.723	∞	6.819×10^{8}	56.64
0.197	0	50.58	6.889	∞	9.764×10^{8}	61.51
0.197	0	100.8	6.816	∞	1.688×10^{9}	72.73
0.197	0	199.8	6.2	∞	3.371×10^{9}	89
0.197	0	299.3	5.474	∞	5.578×10^{9}	103

continued on next page

h (m)	RPM	Power (W)	Pr	E	Ra	Nu
0.197	0	401	4.509	∞	1.099×10^{10}	98.6
0.197	0.123	10.84	6.937	9.943×10^{-4}	2.916×10^{8}	43.41
0.197	0.123	50.67	6.89	9.883×10^{-4}	9.691×10^{8}	62.06
0.197	0.123	101	6.842	9.822×10^{-4}	1.676×10^{9}	72.74
0.197	0.123	200.1	6.336	9.177×10^{-4}	3.26×10^{9}	88
0.197	1.23	10.86	6.898	9.893×10^{-5}	2.771×10^{8}	46.38
0.197	1.23	30.83	6.912	9.911×10^{-5}	6.299×10^{8}	57.66
0.197	1.23	50.78	6.909	9.907×10^{-5}	9.386×10^{8}	63.79
0.197	1.23	101.2	6.873	9.861×10^{-5}	1.623×10^{9}	74.44
0.197	1.23	200.2	6.353	9.2×10^{-5}	3.216×10^{9}	88.73
0.197	3.075	10.84	6.964	3.991×10^{-5}	2.624×10^{8}	47.82
0.197	3.075	30.84	6.947	3.982×10^{-5}	5.938×10^{8}	60.45
0.197	3.075	50.7	6.95	3.984×10^{-5}	8.831×10^{8}	66.74
0.197	3.075	101.1	6.921	3.969×10^{-5}	1.548×10^{9}	76.7
0.197	3.075	200.2	6.416	3.712×10^{-5}	3.054×10^{9}	91.47
0.197	12.3	10.85	6.935	9.938×10^{-6}	2.762×10^{8}	45.9
0.197	12.3	30.83	6.942	9.946×10^{-6}	5.737×10^{8}	62.66
0.197	12.3	50.69	6.967	9.978×10^{-6}	8.353×10^{8}	70.14
0.197	12.3	100.6	6.976	9.99×10^{-6}	1.442×10^{9}	80.37
0.197	12.3	150.6	6.948	9.953×10^{-6}	2.015×10^{9}	86.95
0.197	12.3	201	6.444	9.314×10^{-6}	2.936×10^{9}	94.63
0.197	12.3	299.9	5.509	8.109×10^{-6}	5.221×10^{9}	109
0.197	41.01	10.33	6.84	2.945×10^{-6}	6.037×10^{8}	20.66
0.197	41.01	14.94	6.823	2.939×10^{-6}	7.139×10^{8}	25.41
0.197	41.01	19.96	6.819	2.937×10^{-6}	8.006×10^{8}	30.32
0.197	41.01	24.7	6.91	2.972×10^{-6}	8.634×10^{8}	33.73
0.197	41.01	29.94	6.992	3.003×10^{-6}	9.316×10^{8}	36.83
0.197	41.01	40.09	7.012	3.01×10^{-6}	1.06×10^{9}	43.04
0.197	41.01	50.04	7.037	3.02×10^{-6}	1.178×10^{9}	47.91
0.197	41.01	74.76	7.009	3.009×10^{-6}	1.481×10^{9}	57.49
0.197	41.01	101.2	6.991	3.002×10^{-6}	1.783×10^{9}	65.08
0.197	41.01	150.6	6.814	2.935×10^{-6}	2.436×10^{9}	75.31
0.197	41.01	201	6.418	2.784×10^{-6}	3.017×10^{9}	92.88
0.197	41.01	192.2	6.242	2.717×10^{-6}	3.496×10^{9}	81.33
0.197	41.01	299.8	5.451	2.41×10^{-6}	5.515×10^{9}	105.2
0.197	41.01	284.9	5.297	2.35×10^{-6}	6.422×10^{9}	90.52
0.197	41.01	400.2	4.539	2.051×10^{-6}	1.063×10^{10}	100.6

REFERENCES

Hirst, W & Cox, R 1976 The construction and analysis of sucrose gradients for use with zonal rotors. *Biochemical Journal* **159**, 259–265.

Johnston, H & Doering, C 2009 Comparison of turbulent thermal convection between conditions of constant temperature and constant flux. *Physical Review Letters* **102**, 064501–4.

King, E, Stellmach, S, Noir, J, Hansen, U & Aurnou, J 2009 Boundary layer control of rotating convection systems. *Nature* **457** (7227), 301–304.

King, E M 2009 An investigation of planetary convection: The role of boundary layers. PhD thesis, University of California, Los Angeles.

Lide, David R. 2000 *Handbook of Chemistry and Physics*. CRC Press.

Lopez, J & Marques, F 2009 Centrifugal effects in rotating convection: nonlinear dynamics. *Journal of Fluid Mechanics* **628**, 269–297.

Verzicco, R 2004 Effects of nonperfect thermal sources in turbulent thermal convection. *Physics of Fluids* **16** (6), 1965–1979.